Journal of Catalysis **187,** 139–150 (1999)
Article ID jcat.1999.2588, available online at http://www.idealibrary.com on IDEAL®

Hydrodesulfurization of Benzothiophene over Zeolite-Supported Catalysts Prepared from Mo and Mo–Ni Sulfide Clusters

Mitsugu Taniguchi,* Daichi Imamura,* Hiromi Ishige,* Youichi Ishii,† Takashi Murata,† Masanobu Hidai,† and Takashi Tatsumi*,[1]

*Engineering Research Institute, School of Engineering, The University of Tokyo, Yayoi, Tokyo 113-8656, Japan; and †Department of Chemistry and Biotechnology, Graduate School of Engineering, The University of Tokyo, Hongo, Tokyo 113-8656, Japan

Received February 22, 1999; revised June 4, 1999; accepted June 6, 1999

Molybdenum sulfide cluster $[Mo_3S_4(H_2O)_9]^{4+}$ and nickel–molybdenum bimetallic sulfide cluster $[Mo_3NiS_4Cl(H_2O)_9]^{3+}$ were incorporated into zeolites NaY, HUSY, NaHβ, Na-mordenite (NaMOR), and KL by aqueous ion exchange. EXAFS data revealed that the structure of the molybdenum sulfide cluster remained virtually intact after ion exchange. However, the incomplete cubane-type structure of the cluster might be lost after thermal treatment at 573 K. The structure of the cluster in Mo_3S_4/NaY and Mo_3S_4/KL seems to have changed to the MoS_2-like structure through the hydrodesulfurization (HDS) reaction, although a considerably high level of dispersion was kept. Mo_3S_4 cluster catalysts loaded on NaMOR and KL exhibited a higher level of activity for HDS of benzothiophene than Mo_3S_4 catalysts loaded on the other zeolites. Benzene was formed through acid-catalyzed dealkylation of ethylbenzene, the primary HDS product. Alkylation of benzothiophene with alkenes derived from the cracking of decane as the solvent also occurred. The acidity seems to be produced through the ion exchange and reduction of cationic clusters during activation. Over HUSY- and NaHβ-supported catalysts benzene was the major HDS product. Nickel incorporation into the Mo_3S_4 zeolite catalysts remarkably enhanced the HDS activity. Introduction of the Mo_3NiS_4 core into zeolite as a precursor resulted in catalysts with higher HDS activity than that of Mo_3S_4 core and Ni^{2+} independently; it is conceivable that the intimate interaction between nickel and molybdenum in the precursor is effective at producing active species. © 1999 Academic Press

Key Words: **hydrodesulfurization; zeolites; molybdenum; nickel; sulfide; cluster.**

INTRODUCTION

Recently, the demand for deep hydrodesulfurization (HDS) of light oil has increased and a number of attempts have been made to prepare new catalysts for HDS. The key problem in the deep desulfurization of light oil is the low reactivity of 4-methyldibenzothiophene and 4,6-dimethyldibenzothiophene since the methyl group(s) in the 4 and/or 6 positions of dibenzothiophene hinders the sulfur from approaching the active sites on catalysts (1, 2). All the processes of HDS of petroleum feedstocks have been performed on catalysts of the same type, based on molybdenum (or tungsten) sulfide supported on high-surface-area γ-aluminas with cobalt or nickel added as a promoter (3, 4). The acidic property of zeolites might be capable of activating the alkyl-substituted dibenzothiophenes by isomerizing or eliminating the alkyl groups in the thiophenic rings (5, 6). Therefore, it is conceivable that zeolite-supported molybdenum with nickel or cobalt as a promoter will be a promising catalyst for potential application to the deep HDS reactions.

Most of the molybdenum catalysts loaded on zeolites are prepared by impregnating zeolites with an ammonium heptamolybdate (AHM) solution (7–9). The impregnation method results mostly in the loading of molybdenum species on an external surface, since the anionic or neutral complexes will not penetrate into the zeolite pores in the presence of water (7). Furthermore, the crystallinity of AHM/zeolite catalysts tends to decrease during calcination (8, 9). To overcome these disadvantages, vapor-phase adsorption of the $Mo(CO)_6$ complex has been employed for the preparation of zeolite-supported molybdenum catalysts (10, 11). Okamoto *et al.* have prepared highly dispersed molybdenum sulfide catalysts from $Mo(CO)_6$ encaged in zeolites and showed that the catalysts are more active for HDS of thiophene than that obtained by impregnation of zeolites with AHM solution (10). Although these methods can be used to load molybdenum into zeolite pores, the following thermal treatment may lead to migration of molybdenum and destruction of the zeolite structure (11).

Although ion exchange would be an ideal method for loading active metal species onto zeolite supports with high dispersion, few cationic forms are available as simple salts of molybdenum of high oxidation state. Therefore, few studies have succeeded in introducing cationic

[1] To whom correspondence should be addressed at present address: Division of Materials Science and Chemical Engineering, Faculty of Engineering, Yokohama National University, 79-5 Tokiwadai, Yokohama 240-8501, Japan. Fax: (+81-45) 339 3943. E-mail: ttatsumi@ynu.ac.jp.

0021-9517/99 $30.00

molybdenum compounds into zeolites by ion exchange (12–15). Dai and Lunsford reported the preparation of molybdenum/HY by solid–solid ion exchange using $MoCl_5$ (12). Johns and Howe prepared molybdenum loaded H-mordenite by vapor–phase adsorption of $MoOCl_4$ (13) and molybdenum loaded NaY by aqueous ion exchange with MoO_2Cl_2 (14). Ward *et al.* prepared NaY containing a uniform distribution of molybdenum by aqueous ion exchange using Mo_2(ethylenediamine)$_4Cl_4$ as precursor (15). In these studies zeolite Y (NaY, HY) was generally used as the support. The influence of zeolite types on the property of molybdenum/zeolite catalysts is an interesting subject.

A molybdenum (IV) sulfide cluster with incomplete cubane-type structure $[Mo_3S_4(H_2O)_9]^{4+}$ (**1**) (Fig. 1) has been prepared and studied extensively (16–18). In cluster **1**, molybdenum has octahedral geometry and binds to one μ_3-S, two μ_2-S, and three water ligands. Cluster **1** is cationic and stable in water and air; we have found that cluster **1** can be loaded into zeolites by aqueous ion exchange with its structure preserved (19). Using cluster **1** as a precursor for the molybdenum catalyst has several advantages as follows. Molybdenum species can be loaded into zeolites with high dispersion by ion exchange. The neutral ligand of cluster **1** is water, which can be easily removed by mild heating without high-temperature calcination resulting in migration of molybdenum species to the external zeolite surface and destruction of the zeolite crystal structure (11). Moreover, presulfiding of the catalyst is not necessary; the conventional molybdenum sulfide catalysts were usually prepared by presulfiding molybdenum oxide catalysts (20).

Cluster **1** is easily converted to bimetallic sulfide clusters with cubic Mo_3MS_4 cores (M = Fe, Co, Ni, Cu, Pd, etc.) (21–29), which are of considerable interest in connection with potential application to a variety of catalytic reactions. Mixed metal clusters with a Mo_3PdS_4 core showed intriguing reactivities at the Pd site toward alkenes, CO, isonitriles, and alkynes (26–29). It is expected that the mixed metal clusters could also be incorporated into zeolites by ion exchange and promote unique catalytic reactions. In particular, the nickel–molybdenum bimetallic sulfide cluster ($[Mo_3NiS_4Cl(H_2O)_9]^{3+}$) (**2**) (22) (Fig. 1) is of great interest as a precursor for Mo–Ni-based HDS catalysts because of the existence of Mo–S–Ni linkage in cluster **2**. Two representative models have been proposed for the structure of HDS active sites. One is the Co(Ni)–Mo–S model, in which cobalt or nickel interacts with molybdenum species (30). In the other model the cobalt or nickel site activates hydrogen and the molybdenum site catalyzes the desulfurization (31). Assuming the former model, we considered cluster **2** as a suitable precursor for HDS catalysts. Although a large number of research studies have examined the method of catalyst preparation, to the best of our knowledge, there has been no preceding report in which nickel–molybdenum mixed sulfide was loaded successfully.

We have already reported that the molybdenum and nickel–molybdenum sulfide clusters loaded onto zeolites (Mo_3S_4/zeolites, Mo_3NiS_4/zeolites) exhibit an interesting catalytic performance. The Mo_3S_4/zeolites and the Mo_3NiS_4/zeolites catalyzed CO hydrogenation, producing hydrocarbons, especially ethane and ethylene at high selectivity of 60% (19, 32). KCl-added Mo_3S_4/zeolites produced a significant amount of alcohols (33). The Mo_3NiS_4/NaY catalyst showed much higher activity for HDS of benzothiophene than the Mo_3S_4/NaY catalyst (34, 35). For both reactions KL as a carrier was found to give catalysts with superior activity. Here we report on the detailed study on the influence of zeolite structure in the HDS of benzothiophene with the Mo_3S_4/zeolite catalysts and the effect of the nickel addition method on the performance of the Mo–Ni-based HDS catalysts.

EXPERIMENTAL PROCEDURES

Catalyst Preparation

The chloride salt of cluster **1** was synthesized by the method reported by Shibahara *et al.* (17) using $(NH_4)_2MoS_4$ (Kanto Chemical) as a starting material. Cluster **1** was loaded on zeolites with 12-membered ring structure, NaY (Nikka Seiko, SK-40; Si/Al = 2.3), HUSY (Tosoh, TSZ-330HUA; Si/Al = 3.1), KL (Tosoh, TSZ-500KOA; Si/Al = 3.1), NaHβ (Tosoh, Tβ-111; Si/Al = 12.8, Na/Al = 0.36), and NaMOR (Tosoh, TSZ-640NAA; Si/Al = 9.6), by aqueous ion exchange to give Mo_3S_4/zeolite. The detailed procedure of catalyst preparation will be described elsewhere (36). The catalysts were dried at 383 K overnight and not calcined.

The chloride salt of cluster **2** was synthesized from cluster **1** and $NiCl_2 \cdot 6H_2O$ (Koso Chemical), according to the reported method (22). The cluster **2** obtained was similarly loaded onto zeolites NaY, KL, and NaMOR to give Mo_3NiS_4/zeolites. It should be noted that cluster **2** was handled under N_2 because the $Mo_3NiS_4^{4+}$ core is slowly air-oxidized, according to (22):

$$2Mo_3NiS_4^{4+} + O_2 + 4H^+ \rightarrow 2Mo_3S_4^{4+} + 2Ni^{2+} + 2H_2O. \quad [1]$$

As a control catalyst, Ni + Mo_3S_4/KL was prepared by ion-exchanging Mo_3S_4/KL with an aqueous solution of $Ni(NO_3)_2 \cdot 6H_2O$ (Koso Chemical) (Ni/Mo = 1/3). AHM/NaY and AHM/KL were prepared by impregnating NaY and KL with an aqueous solution of $(NH_4)_6Mo_7O_{24} \cdot 4H_2O$ (AHM) (Nacalai Tesque) followed by drying at 383 K overnight and calcination in air at 773 K for 4 h. AHM + Ni/NaY and AHM + Ni/KL were prepared by ion-exchanging NaY and KL with an aqueous solution of $Ni(NO_3)_2 \cdot 6H_2O$, followed by impregnation of the ion-exchanged zeolites

with an aqueous solution of AHM and calcination in air at 773 K for 4 h.

Characterization

Molybdenum, sodium, and potassium concentrations in the filtrate obtained after ion exchange were determined on a Nippon Jarrell-Ash ICAP-575 ICP spectrophotometer. Sulfur contents were determined by the LECO method. Chlorine contents of the catalysts were determined by ion chromatography. Thermogravimetry (TG) and differential thermal analyses (DTA) were performed on a Shinku-Riko TGD 7000 thermogravimeter in N_2 flow. The temperature ramping rate was 5 K min^{-1}. UV–visible spectra were recorded on a Hitachi U-4000 spectrophotometer. The Mo K-edge X-ray absorption spectra were collected on a Rigaku R-EXAFS 2100S spectrometer (30 kV, 280 mA, W filament, Cu target) using a Ge(400) crystal monochromator at room temperature. The Ni K-edge X-ray absorption spectrum of cluster **2** and the Ni K-edge X-ray fluorescence spectra of the supported catalysts were also collected (16 kV, 500 mA, LaB_6 filament, Mo target) using a Ge(440) crystal monochromator at room temperature. The samples were pressed into self-supported disks of 20 mm in diameter and subjected to analysis. Because of the instability of cluster **2** against air, cluster **2** and Mo_3NiS_4/KL were kept under a N_2 atmosphere during the measurement. At least five scans were done and averaged spectra were obtained. The EXAFS data analysis was carried out by utilizing REX, an EXAFS data analysis software program provided by Rigaku. X-ray photoelectron spectroscopy (XPS) measurements of the catalysts were performed using a VG scientific ESCALAB 220I spectrometer at 15 kV and 20 mA with an Al anode. Binding energies were referenced to C 1*s* of 285.0 eV for MoS_2 and the nickel–molybdenum cluster and to Al 2*p* of 75.0 eV for zeolite. The *in situ* XPS spectra of the catalysts pretreated in H_2 flow at 573 K were also recorded.

HDS Reaction

The activity of the catalysts for the benzothiophene hydrodesulfurization reaction was measured in a flow-type fixed-bed reactor. The reaction conditions were as follows: temperature 573 K, total pressure 3.0 MPa, catalyst 0.2 g, W/F = 378 or 37.8 g-cat · h/mol S (concentration of sulfur in decane 0.5 or 5.0 wt% S), and flow rate of hydrogen 3.42 L/h. The catalysts were pretreated in He at 573 K for 0.5 h and then in H_2 at 573 K for 0.5 h. Neither calcination nor sulfiding treatment was conducted except for AHM-supported zeolite catalysts; AHM-supported zeolites were calcined at 773 K for 2 h and presulfided with a mixture of 5% H_2S in H_2 at 673 K for 2 h before the reaction.

RESULTS AND DISCUSSION

Ion Exchange of Zeolites with the Clusters

The chemical compositions of the prepared catalysts are summarized in Table 1. Clusters **1** and **2** were loaded on all the zeolites with a 12-membered ring accompanied by elution of a corresponding counter cation (Na or K) to the filtrate except for HUSY. The Cl/Mo ratio in the samples decreased from 1.33 in the original cluster **1** to 0–0.34, depending on the samples, in the cluster-loaded zeolites. These results show the zeolites were ion-exchanged with these cluster cations. Although the pH of the solution during ion exchange was relatively low (pH 3.1–4.7 as shown in Table 1), the crystallinity of the ion-exchanged zeolites was estimated by XRD to be higher than 70%.

The size of the incomplete Mo_3S_4 cubane core of cluster **1**, shown in Fig. 1, was estimated to be 0.63 nm from

TABLE 1

Elemental Analyses of Mo_3S_4 and Mo_3NiS_4/Zeolite Catalysts

Catalyst	Pore size (nm)[a]	Si/Al ratio	Loaded Mo (wt%)	% loaded Mo (%)[b]	Na (K) released (mol/mol)[c]	Cl/Mo ratio	% occupied ion-exchange sites	pH after ion exchange
Mo_3S_4/NaY	0.74***	2.3	5.0	100	4.6	0.11	21	4.6
Mo_3S_4/HUSY	0.74***	3.1	2.3	92	—	0.34	8.7	4.2
Mo_3S_4/NAHβ	0.76 × 0.64** 0.55 × 0.55*	12.8	2.5	100	3.6	0.21	29	3.3
Mo_3S_4/KL	0.71*	3.1	2.1	74	4.4	0.00	10	3.2
Mo_3S_4/NaMOR	0.65 × 0.70* 0.26 × 0.57*	9.6	2.0	78	4.5	0.15	18	3.1
Mo_3NiS_4/NaY	0.74***	2.3	5.0	99	4.2	0.12	21	4.7
Mo_3NiS_4/KL	0.71*	3.1	1.8	72	3.6	0.21	4.8	3.4
Mo_3NiS_4/NaMOR	0.65 × 0.70* 0.26 × 0.57*	9.6	1.6	63	3.2	0.37	12	3.1

[a] The number of asterisks indicates whether the channel system is one-, two-, or three-dimensional. Adapted from Ref. (37).
[b] Fraction of Mo loaded based on Mo added to the solution.
[c] Mol Na (K) released into the solution per mole of cluster loaded.

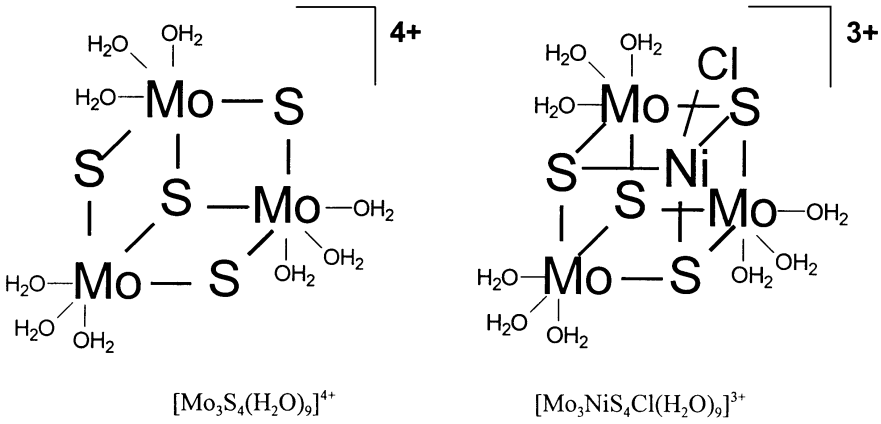

FIG. 1. Structure of incomplete cubane-type molybdenum sulfide cluster $[Mo_3S_4(H_2O)_9]^{4+}$ (**1**) and complete cubane-type nickel-molybdenum bimetallic sulfide cluster $[Mo_3NiS_4Cl(H_2O)_9]^{3+}$ (**2**).

the crystallographic data reported by Akashi *et al.* (18) and the ionic radius of S^{2-} (0.184 nm) and Mo^{4+} (0.064 nm). This cluster size is smaller than the pore opening (0.74 nm) (37) of supercages of the FAU structure. Hence cluster **1** seems to be able to enter the NaY pore inside the crystals. The S/Mo ratio of Mo_3S_4/NaY remained unchanged after ion exchange. The released sodium ion in the filtrate was 4.6 times (ideally $4 - 0.11 \times 3 = 3.7$ times) as much as the loaded cluster **1**. This slight excess of released sodium over the supported cluster may be due to the acidity of the cluster salt. Brønsted acid sites should be produced during ion exchange (33). For Mo/HUSY, cluster **1** amounting to 2.5 wt% (as molybdenum metal) of HUSY was added to the suspension of HUSY; the filtrate remained brown-colored and 92% of the molybdenum was loaded onto HUSY.

In the preparation of Mo_3S_4/KL, Mo_3S_4/NaMOR, and Mo_3S_4/NaHβ, the addition of **1** was stopped when the pH of the suspension was lowered to about 3 in order to avoid decomposition of the zeolite structure. Since the diameters of the pore openings of these zeolites (Table 1) are slightly larger than the size of cluster **1** (0.63 nm), cluster **1** seems to be able to enter the pores of the zeolites. The molybdenum loading of Mo_3S_4/NaHβ was 2.5 wt%; all added cluster was loaded despite the high Si/Al ratio of NaHβ.

Mo_3S_4/KL and Mo_3S_4/NaMOR incorporated only 2.1 and 2.0 wt% (74 and 78% of the added molybdenum clusters) molybdenum. The difficulty in ion-exchanging KL and NaMOR should not be due to deficiency of ion-exchange sites; the loaded amount of cluster cation corresponds to only 10 and 18% of the ion-exchange capacity of KL and NaMOR, respectively. These sluggish ion exchanges would be due to the 1-dimensional pore structure of KL and NaMOR. It is conceivable that once cluster **1** is incorporated into a 1-dimensional channel of KL and MOR and present at a site near the external surface, the sites deep in the channel are hardly accessible to another cluster. The location of the molybdenum cluster in zeolite particles will be discussed elsewhere (36).

Cluster **2** was also introduced into NaY, KL, and NaMOR by ion exchange. The ion-exchange behavior of the zeolites with cluster **2** was similar to that with cluster **1**. The Cl/Mo ratio of Mo_3NiS_4/NaY and Mo_3NiS_4/KL was 0.12 and 0.21, respectively, and less than the Cl/Mo ratio of the cubic core of cluster **2** (0.33). Dimmock *et al.* reported that the coordinating chlorine in cluster **2** was replaced with water in a solution with low Cl^- concentration (22). Thus the chlorine ligand might be partly exchanged with water during washing, resulting in formation of $[Mo_3NiS_4(H_2O)_{10}]^{4+}$ as expressed by

$$[Mo_3NiS_4Cl(H_2O)_9]^{3+} + H_2O \rightarrow [Mo_3NiS_4(H_2O)_{10}]^{4+} + Cl^-. \quad [2]$$

EXAFS Analysis 1—Structure of Mo Sulfide Cluster Loaded on Zeolites

We have carried out EXAFS analyses of cluster **1** and zeolite-supported **1**. Figure 2 shows the Mo K-edge EXAFS spectra of cluster **1**, Mo_3S_4/NaY, and Mo_3S_4/KL. The spectra of Mo_3S_4/NaY and Mo_3S_4/KL were similar in amplitude and periodicity to the spectrum of cluster **1**, suggesting that the molybdenum species in Mo_3S_4/NaY and Mo_3S_4/KL kept the original incomplete cubane-type structure. The Fourier transforms of EXAFS data and the curve-fitting results are shown in Fig. 3 and Table 2, respectively. The structural parameters of $[Mo_3S_4(H_2O)_9](CH_3C_6H_4SO_3)_4$, the *p*-toluenesulfonate salt of cluster **1**, determined by single crystal X-ray structural analysis (18) are also shown in Table 2. The structural parameters of cluster **1** determined by curve fitting were in good agreement with the crystallographic data. Structural parameters of the Mo species in Mo_3S_4/NaY and Mo_3S_4/KL showed virtually no change in the Mo–O, Mo–S, and Mo–Mo distances and a slight change in the coordination numbers of Mo–O and Mo–S, indicating that there was no significant structural difference between cluster **1** and the molybdenum species in Mo_3S_4/NaY and

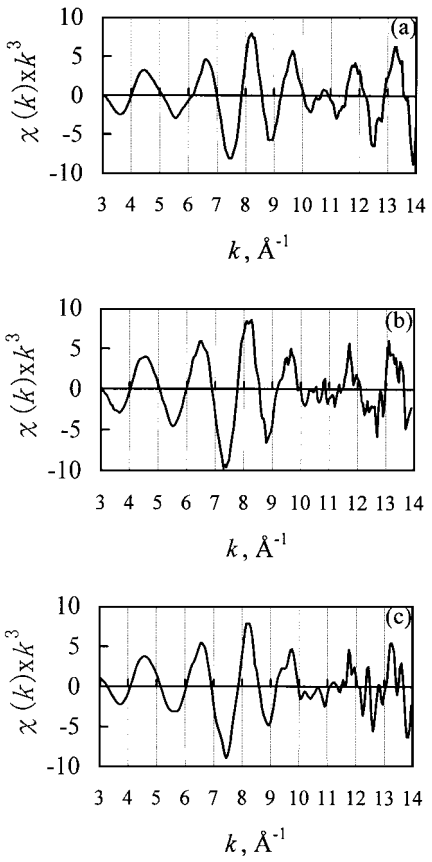

FIG. 2. Mo K-edge EXAFS spectrum of (a) the chloride salt of **1**, (b) Mo_3S_4/NaY, and (c) Mo_3S_4/KL.

Mo_3S_4/KL. The reason for the slight decrease in the coordination number of Mo–Mo for Mo_3S_4/KL could be the unsatisfactory S/N ratio of the EXAFS spectrum in the range of k = 10–14 Å^{-1}, partly due to the relatively low molybdenum loading in Mo_3S_4/KL. However, it can be concluded from these EXAFS data that the structure of cluster **1** remained virtually intact after ion exchange.

After treatment at 573 K in He flow, however, the color of NaY changed from brown to black, suggesting a change in the structure of the cluster. The curve-fitting results of the EXAFS data revealed the decrease in the coordination numbers for all interactions compared to the original Mo_3S_4/NaY. The decrease in the coordination number is not due to the loss of sulfur atoms but to the disordering of each interaction since elemental analysis showed no decrease in sulfur amount after thermal treatment at 573 K. Although the incomplete cubane-type structure of cluster **1** might be lost after the thermal treatment at 573 K, no significant peak corresponding to the Mo–Mo and Mo–S shell was observed in the Fourier transforms of the EXAFS spectrum.

The Fourier transforms of the catalysts used for the HDS reaction of benzothiophene (Figs. 3e and 3f) showed slight increases in the Mo–S and Mo–Mo distances. The curve-fitting results suggested that the Mo–S and Mo–Mo distances were strikingly similar to those in MoS_2, known as the active molybdenum species in the conventional HDS catalysts, while the coordination numbers were much smaller than those for MoS_2 (39). Thus it seems that the structure of cluster **1** in Mo_3S_4/NaY and Mo_3S_4/KL changed to the MoS_2-like structure through the HDS reaction. The structure of the molybdenum species on the used catalysts were dependent on zeolite; Mo_3S_4/KL exhibited higher coordination numbers in Mo–S and Mo–Mo interactions than Mo_3S_4/NaY. The molybdenum species in the used Mo_3S_4/NaY seems to remain highly dispersed, resulting in lower coordination numbers in Mo–S and Mo–Mo distances. Clusters **1** localized on and near the external surface of the KL particle would aggregate more easily to form molybdenum sulfide particles (36).

UV–Visible Spectra—Structure of MoNi Sulfide Cluster

The UV–visible spectrum of Mo_3NiS_4/KL (Fig. 4b) showed a band at 240 nm, characteristic of cluster **2** (Fig. 4a), suggesting virtual retention of the structure of cluster **2** during ion exchange. For Ni + Mo_3S_4/KL (Fig. 4c) this band was hardly observed. Mo_3NiS_4/KL also showed a shoulder band at 390 nm, characteristic of cluster **1**, as shown in Fig. 4d; cluster **2** might be partly decomposed to the incomplete cubane-type cluster **1** after ion exchange according to Eq. [1].

EXAFS Analysis 2—Structure of MoNi Sulfide Cluster Loaded on Zeolite

The radial distance of Mo–Mo and Mo–Ni in $[Mo_3NiS_4(H_2O)_{10}]^{4+}$ is 0.274 and 0.264 nm, respectively (23). Since

TABLE 2

Curve-Fitting Results for $[Mo_3S_4(H_2O)_9]$ Cluster and Mo_3S_4/Zeolites

Sample	Treatment	Mo–S		Mo–Mo		Mo–O	
		N^a	R (nm)^b	N^a	R (nm)^b	N^a	R (nm)^b
Cluster **1**^{c}	—	3.0	0.230	2.0	0.274	3.0	0.218
Cluster **1**	—	2.9	0.230	2.0	0.274	3.3	0.218
Mo_3S_4/NaY	—	3.5	0.232	2.0	0.276	3.9	0.217
Mo_3S_4/KL	—	3.0	0.231	1.7	0.278	2.7	0.216
Mo_3S_4/NaY	He, 573 K	1.2	0.238	0.6	0.276	1.3	0.214
Mo_3S_4/NaY	HDS used	2.3	0.239	0.59	0.318	—	—
Mo_3S_4/KL	HDS used	3.6	0.241	2.1	0.315	—	—
Mo/Al_2O_3^{d}	Sulfurized	6.2	0.241	3.1	0.315	—	—
MoS_2^{e}	—	6.0	0.241	6.0	0.316	—	—

[a] Coordination number.

[b] Radial distance from the absorber to be backscatter atom.

[c] Crystallographic data from Ref. (18). The radial distance between Mo and S was determined by taking an average of one Mo–(μ_3-S) (0.2337 nm) and two Mo–(μ_2-S) (0.2283 nm).

[d] Conventional sulfurized Mo/Al_2O_3 catalyst. Adopted from Ref. (38).

[e] Adopted from Ref. (38).

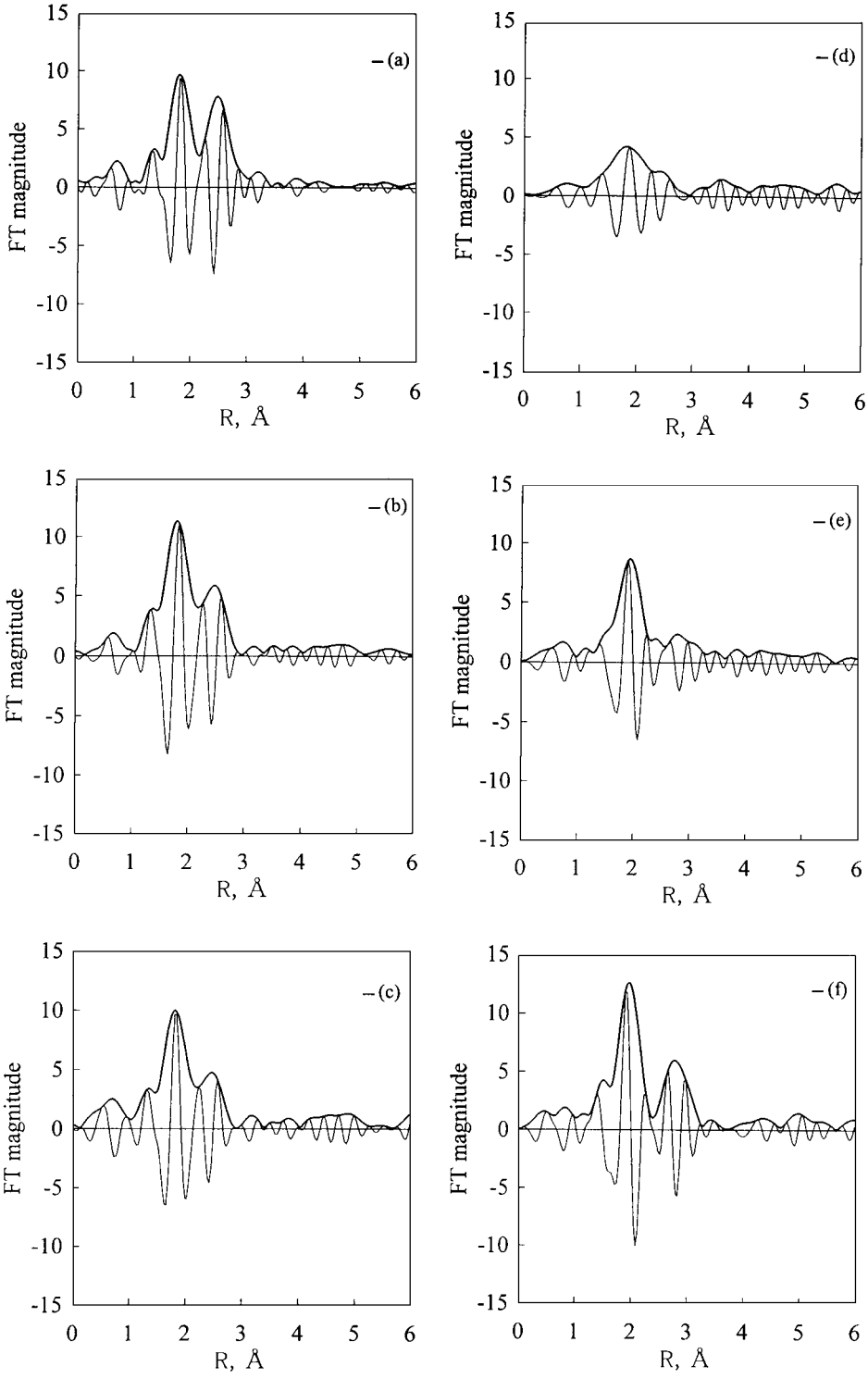

FIG. 3. Fourier transforms of Mo K-edge EXAFS data of (a) the chloride salt of **1**, (b) Mo_3S_4/NaY, (c) Mo_3S_4/KL, (d) Mo_3S_4/NaY after treated in He flow at 573 K, (e) Mo_3S_4/NaY after HDS of benzothiophene, and (f) Mo_3S_4/KL after HDS of benzothiophene.

these radial distances are similar and scattering of nickel is weak compared to that of molybdenum, it is quite difficult to determine the structural parameters of Mo–Ni coordination from Mo K-edge EXAFS. Therefore, we measured Ni K-edge EXAFS to obtain the structural parameters around the nickel atom in Mo_3NiS_4/zeolites. Figure 5 shows the Fourier transforms of EXAFS data of cluster **2** and Mo_3NiS_4/KL after ion exchange (not thermally treated).

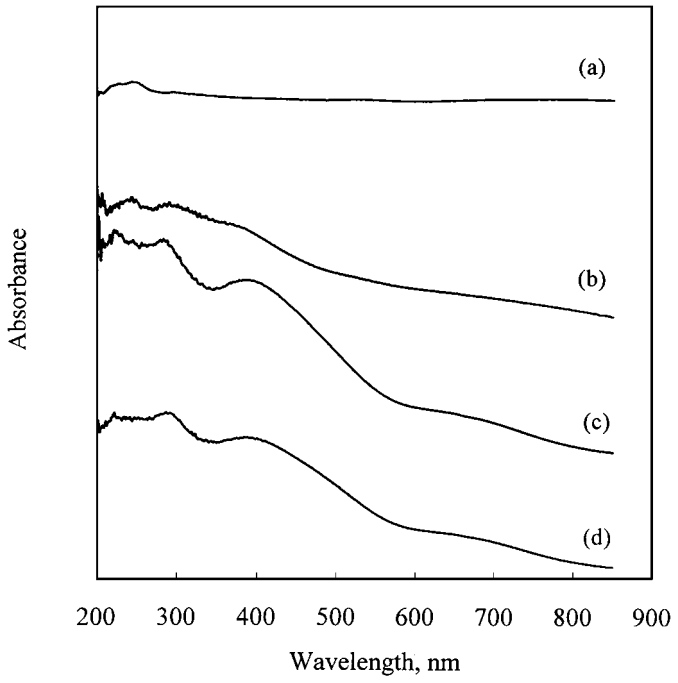

FIG. 4. UV–visible spectra of (a) physical mixture of NaY and the chloride salt of **2**, (b) Mo_3NiS_4/KL, (c) Ni + Mo_3S_4/KL, and (d) Mo_3S_4/KL.

The curve-fitting results are shown in Table 3. Because the distances of Ni–S and Ni–Cl are very close, it is impossible to distinguish these interactions; the Ni–Cl and Ni–S shells were combined in the analysis. The Ni–Mo distance of Mo_3NiS_4/KL was virtually the same as that of cluster **2**, suggesting the retention of the cubane-type structure of cluster **2** in Mo_3NiS_4/KL. The Ni–Mo coordination number was decreased during ion exchange. The reason for this decrease must be partial destruction of cluster **2** according to Eq. [1] as revealed by the UV–visible spectrum of Mo_3NiS_4/KL (Fig. 4).

In contrast, the peak corresponding to the Ni–Mo shell was not observed in the Fourier transforms of Ni + Mo_3S_4/KL. Nickel in Ni + Mo_3S_4/KL seems to be present as $Ni(H_2O)_6^{2+}$ in the ion-exchange site without significant interaction with molybdenum.

The Fourier transforms of Mo K-edge EXAFS of cluster **2** and Mo_3NiS_4/KL are shown in Fig. 6. As mentioned above, it is quite difficult to determine the structural parameters of the Mo–Ni shell from the Mo K-edge EXAFS. Therefore, we analyzed the Mo K-edge EXAFS data by applying the distance and coordination number of the Ni–Mo shell obtained from Ni K-edge EXAFS analyses to the Mo K-edge EXAFS analysis of cluster **2** and Mo_3NiS_4/KL as fixed parameters. Thus obtained curve-fitting results are shown in Table 4. The structural parameters of cluster **2** determined by curve fitting are in good agreement with the crystallographic data. Structural parameters of Mo_3NiS_4/KL showed virtually no change in the Mo–S and Mo–Mo distances and the coordination numbers. The decrease in coordination number of Mo–Ni during the ion exchange must be due to partial destruction of cluster **2** as described above. It can be concluded that the structure of cluster **2** was

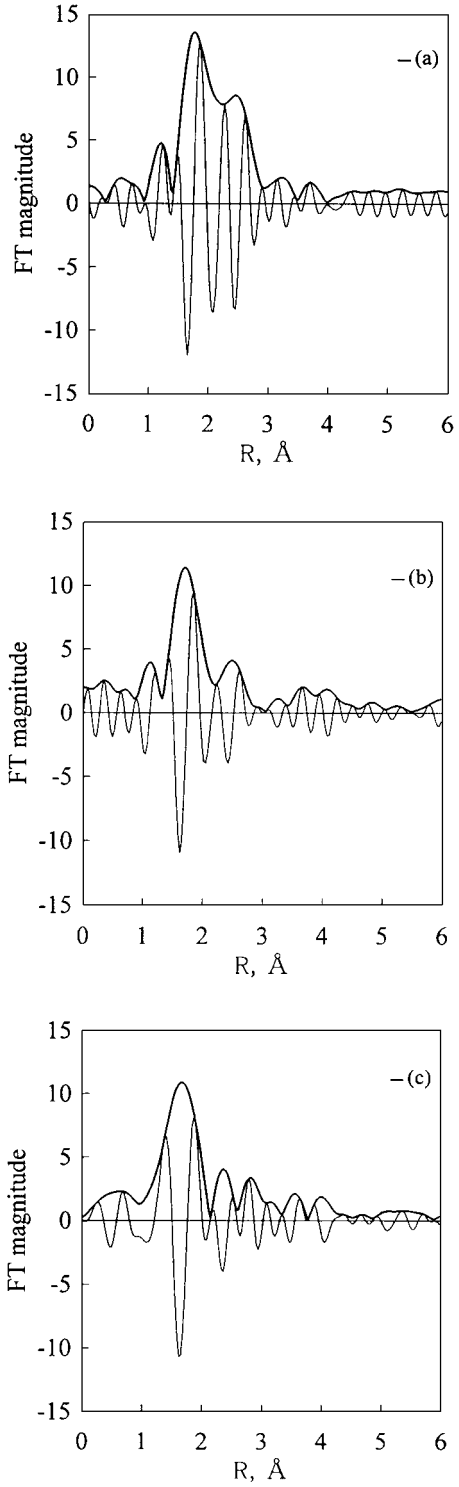

FIG. 5. Fourier transforms of Ni K-edge EXAFS data of (a) the chloride salt of **2**, (b) Mo_3NiS_4/KL, and (c) Ni + Mo_3S_4/KL.

TABLE 3

Curve-Fitting Results of Ni K-Edge EXAFS Data for Cluster 2 and KL Supported Catalysts

Sample	Ni–S		Ni–Mo		Ni–Cl		Ni–O	
	N^a	R^b (nm)	N^a	R^b (nm)	N^a	R^b (nm)	N^a	R^b (nm)
$[Mo_3NiS_4(H_2O)_{10}]^{4+}$ [c]	3.0	0.220	3.0	0.264	—	—	1.0	0.196
$[Mo_3NiS_4(Hnta)(nta)_2Cl]^{5-}$ [d]	3.0	0.222	2.0	0.267	1.0	0.224	—	—
	Ni–S (Cl)		Ni–Mo				Ni–O	
	N^a	R^b (nm)	N^a	R^b (nm)			N^a	R^b (nm)
Cluster **2**	2.9	0.222	3.0	0.267			—	—
Mo_3NiS_4/KL	2.5	0.217	1.9	0.269			—	—
Ni + Mo_3S_4/KL	—	—	—	—			5.4	0.204

[a] Coordination number.
[b] Radial distance from the absorber to the backscatter atom.
[c] Crystallographic data from Ref. (24).
[d] Crystallographic data from Ref. (24). nta, Nitrilotriacetate anion, $N(CH_2COO)^{3-}$.

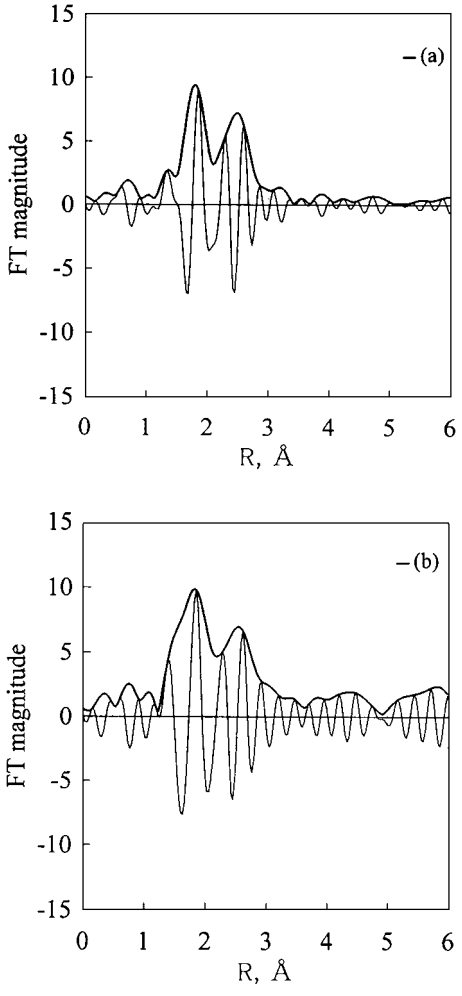

FIG. 6. Fourier transforms of Mo K-edge EXAFS data of (a) the chloride salt of **2** and (b) Mo_3NiS_4/KL.

mostly retained but partly decomposed to the incomplete-cubane-type cluster **1** after ion exchange.

XPS Analyses

To study the electronic character of the molybdenum-loaded zeolites, X-ray photoelectron spectra were taken of Mo_3NiS_4/NaY, Mo_3NiS_4/KL, Ni + Mo_3S_4/KL, and AHM + Ni/KL (presulfided). The binding energies are listed in Table 5. The Mo 3*d* binding energies for cluster **2** hardly changed by loading on NaY and KL through ion exchange. The type of zeolite did not significantly affect the Mo 3*d* binding energies. In contrast, the Ni 2*p* binding energy of cluster **2** decreased slightly by loading on NaY and KL through ion exchange. This decrease in the binding energy may be caused by the substitution of water for the chlorine coordinating to Ni, as described above.

The lowering of Mo 3*d* and Ni 2*p* binding energies upon *in situ* treatment with H_2 at 573 K for 2 h indicates that the molybdenum and nickel of the catalysts have been reduced. After HDS reaction, the Mo 3*d* binding energies of Mo_3NiS_4/KL increased to those of MoS_2. This result agrees with the supposition that cluster **1** in Mo_3S_4/KL was sulfided to a MoS_2-like structure after the HDS reaction as described above. After H_2 treatment, no significant difference in the Mo 3*d* and Ni 2*p* binding energies was observed between Mo_3NiS_4/KL and Ni + Mo_3S_4/KL. The decrease in Mo 3*d* binding energies for AHM + Ni/KL after H_2 reduction was smaller than that for the cluster loaded catalysts. This might be due to low reducibility of the molybdenum species with a large particle size on the AHM-derived catalyst.

There was virtually no difference in the Mo 3*d* binding energies among Mo_3NiS_4/KL, Ni + Mo_3S_4/KL, and Ni + AHM/KL after the HDS reaction; the electronic character of molybdenum and nickel in the three catalysts after the

TABLE 4

Curve-Fitting Results of Mo K-Edge EXAFS Data for $[Mo_3NiS_4Cl(H_2O)_9]$ Cluster and Mo_3NiS_4/KL

Sample	Mo–S		Mo–Mo		Mo–Ni		Mo–O	
	N^a	R^b (nm)	N^a	R^b (nm)	N^a	R^b (nm)	N^a	R^b (nm)
$[Mo_3NiS_4(H_2O)_{10}]^{4+}$ [c]	3.0	0.234	2.0	0.276	1.0	0.264	3.0	0.220
$[Mo_3NiS_4(Hnta)(nta)_2Cl]^{5-}$ [d]	3.0	0.235	2.0	0.278	1.0	0.267	—	—
Cluster **2**	3.0	0.230	1.6	0.280	1.0[e]	0.267[e]	3.7	0.221
Mo_3NiS_4/KL	2.8	0.230	2.0	0.280	0.65[e]	0.269[e]	1.2	0.210

[a] Coordination number.

[b] Radial distance from the absorber to the backscatter atom.

[c] Crystallographic data from Ref. (24). The radial distance between Mo and S was determined by taking an average of one Mo–S (0.2349 nm) and two Mo–S (0.2334 nm).

[d] Crystallographic data from Ref. (24). nta, Nitrilotriacetate anion, $N(CH_2COO)^{3-}$. The radial distance between Mo and S was determined by taking an average of one Mo–S (0.2349 nm) and two Mo–S (0.2343 nm).

[e] Taken from the distance and coordination number of the Ni–Mo shell obtained from Ni K-edge EXAFS analyses (Table 3).

HDS reaction was very similar. As will be discussed below, however, there was a marked difference in the activity for the HDS of benzothiophene among the three.

HDS Activity of Mo_3S_4/Zeolites—Influence of Zeolites

The catalysts were tested for the HDS of benzothiophene. Ethylbenzene was obtained as the main product. Other HDS products consisted mainly of benzene, which was produced from ethylbenzene by the acidic function of the catalysts. Dihydrobenzothiophene and other sulfur-containing products such as alkylbenzothiophenes were also formed. The alkylbenzothiophenes are considered to have been produced from unreacted benzothiophene and alkenes that were generated from decane cracking. In all experiments, the benzothiophene conversion and product distribution were practically unchanged after 2 h on stream. Table 6 presents the stabilized activity and selectivity for the HDS of benzothiophene over Mo_3S_4/zeolite catalysts obtained after 4 h on stream. All Mo_3S_4/zeolite catalysts showed higher conversion of benzothiophene than AHM/NaY and AHM/KL catalysts used after presulfiding. Not only Mo_3S_4/HUSY and Mo_3S_4/NaHβ but also Mo_3S_4/NaY, Mo_3S_4/KL, and Mo_3S_4/NaMOR promoted acid-catalyzed reactions to produce benzene and alkylbenzothiophenes. These compounds were not formed in the reaction over AHM/NaY and AHM/KL. Acid sites strong enough to catalyze cracking and alkylation seem to be formed through two pathways: (i) exchange of the counter cations of zeolites such as Na^+ and K^+ with protons during ion exchange because of acidity of the cluster and (ii) reduction of the cluster accompanied by formation of Brønsted acid sites according to the equation

$$Mo_3S_4^{4+} - 4Z^- + x/2\ H_2 \rightarrow Mo_3S_4^{(4-x)+} - (4-x)Z^- + xH^+ - xZ^-, \qquad [3]$$

where Z^- is the ion-exchange site of zeolite. XPS analysis revealed that the Mo_3S_4 cluster was reduced with hydrogen treatment during pretreatment at 573 K as mentioned above. These acid sites could be formed on the molybdenum/zeolite catalysts prepared by impregnation with AHM, since some ion exchange of the Na^+ ions of zeolites with the NH_4 ions of the AHM may occur. In the spectrum of temperature-programmed desorption of ammonia adsorbed on Mo_3S_4/KL activated in helium flow, two well-resolved desorption peaks were observed, a low-temperature peak at about 170°C and a high-temperature peak at ~320°C, the latter indicating that strong acid

TABLE 5

XPS Data for Mo Cluster Catalysts (eV)

Catalyst	Mo3*d*3/2	Mo3*d*5/2	Ni2*p*3/2
$[Mo_3S_4(H_2O)_9]Cl_4$	233.2	230.1	
$[Mo_3NiS_4Cl(H_2O)_9]Cl_4$	233.0	229.9	854.4
MoS_2	232.3	229.2	
Fresh catalysts			
Mo_3NiS_4/NaY	232.9	229.8	854.0
Mo_3NiS_4/KL	232.9	229.9	854.0
Ni + Mo_3S_4/KL	233.1	230.0	854.0
AHM + Ni/KL (sulfurized)[a]	232.5	228.9	854.0
H_2 treated at 573 K			
Mo_3NiS_4/NaY	231.2	228.0	852.8
Mo_3NiS_4/KL	231.3	228.1	853.1
Ni + Mo_3S_4/KL	231.4	228.2	853.1
AHM + Ni/KL	232.0	228.6	852.7
HDS used			
Mo_3NiS_4/KL	232.3	229.1	854.0
Ni + Mo_3S_4/KL	232.3	229.1	854.0
AHM + Ni/KL	232.2	229.0	853.8

[a] Presulfurized in 5% H_2S/H_2 flow for 2 h at 573 K.

TABLE 6

Effect of Zeolites on Hydrodesulfurization of Benzothiophene over Molybdenum Sulfide Cluster Encapsulated into Zeolites

Catalyst	Mo loading (wt%)	Conv. (%)	Yield of HDS products (%)	Selectivity (%)			
				EB[a]	Other HDS products[b]	DHBT[c]	Others[d]
Mo_3S_4/NaY	5.0	53	8.8	8.3	8.3	76	7.4
Mo_3S_4/HUSY	2.3	39	9.8	6.1	19	66	8.7
Mo_3S_4/NaHβ	2.5	37	14	14	24	33	29
Mo_3S_4/KL	2.1	75	33	38	5.6	52	3.8
Mo_3S_4/NaMOR	2.0	62	31	48	2.6	48	0.8
AHM/NaY[e]	5.0	24	10	48	0.0	52	0.0
AHM/KL[e]	2.1	14	7.9	57	0.0	43	0.0

Note. Reaction conditions: 573 K, 3.0 MPa, W/F = 382 g-cat · h/mol S, sulfur content 0.5 wt% in decane.
[a] Ethylbenzene.
[b] Other desulfurized compounds, e.g., benzene and toluene.
[c] Dihydrobenzothiophene.
[d] Other sulfur-containing compounds, e.g., alkylbenzothiophenes.
[e] Presulfurized in 5% H_2S/H_2 flow for 2 h at 573 K.

sites are produced in KL zeolite (33). In contrast, a high-temperature peak was not observed for AHM/KL. Hence ethylbenzene was the sole HDS product on the AHM/NaY and AHM/KL catalysts; benzene and alkylbenzothiophenes were not obtained.

Catalysts supported on proton-type zeolites, HUSY and NaHβ, showed higher selectivity for benzene and alkylbenzothiophenes. Mo_3S_4/NaHβ produced alkylbenzothiophenes and desulfurized compounds other than ethylbenzene at high selectivity of 24 and 29%, respectively; Mo_3S_4/NaHβ remarkably promoted acidic reactions such as cracking, alkylation, and dealkylation.

It is particularly noteworthy that Mo_3S_4/KL and Mo_3S_4/NaMOR exhibited superior HDS activity to other Mo_3S_4/zeolites despite low molybdenum loadings. This result is contrary to what would be expected; the diffusion of reactants and products should be difficult for the zeolites with a 1-dimensional pore structure. The reason for this high level of activity might be due to the site of the active molybdenum species. In Mo_3S_4/KL and Mo_3S_4/NaMOR the molybdenum species must be present on the external surface and/or the site near the external surface of 1-dimensional pore structure as will be reported elsewhere (36). We have found that the zeolite-supported catalysts prepared from the clusters are active for the hydrodesulfurization of 4,6-dimethyldibenzothiophene because of the acidity promoting methyl migration (40). However, it is important to note that the acidity also could lead to cracking, which might make these catalysts unsuitable for the hydrodesulfurization of gas oils.

HDS Activity of Mo_3NiS_4/Zeolite—Influence of Nickel Addition

Table 7 compares the HDS activity and selectivity of the cluster **2**/zeolite catalysts and Ni-Mo/zeolite catalysts

TABLE 7

Influence of Nickel and Molybdenum Source for the HDS Reaction

Catalyst	Mo loading (wt%)	Conv. (%)	Yield of HDS products (%)	Selectivity (%)			
				EB[a]	Other HDS products[b]	DHBT[c]	Others[d]
Mo_3S_4/NaY	5.0	97	93	88	5.3	1.2	5.7
AHM + Ni/NaY[e]	5.0	59	45	72	3.4	23	1.2
Mo_3NiS_4/KL	1.8	94	93	97	1.4	1.3	0.2
AHM + Ni/KL[e]	2.1	43	39	88	1.1	11	0.0

Note. Reaction conditions: 573 K, 3.0 MPa, W/F = 382 g-cat · h/mol S, sulfur content 0.5 wt% in decane.
[a] Ethylbenzene.
[b] Other desulfurized compounds, e.g., benzene and toluene.
[c] Dihydrobenzothiophene.
[d] Other sulfur-containing compounds, e.g., alkylbenzothiophenes.
[e] Presulfurized in 5% H_2S/H_2 flow for 2 h at 573 K.

TABLE 8

Influence of Nickel Addition Method onto Zeolite for the HDS Reaction

Catalyst	Mo loading (wt%)	Conv. (%)	Yield of HDS products (%)	Selectivity (%)			
				EB[a]	Other HDS products[b]	DHBT[c]	Others[d]
Mo_3S_4/KL	2.1	21	3.1	14	1.0	82	2.9
Ni + Mo_3S_4/KL	2.1	32	14	39	2.2	47	12
Mo_3NiS_4/KL	1.8	44	27	61	0.2	27	10

Note. Reaction conditions: 573 K, 3.0 MPa, W/F = 38.2 g-cat · h/mol S, sulfur content 5.0 wt% in decane.
[a] Ethylbenzene.
[b] Other desulfurized compounds, e.g., benzene and toluene.
[c] Dihydrobenzothiophene.
[d] Other sulfur-containing compounds, e.g., alkylbenzothiophenes.

prepared from AHM and $Ni(NO_3)_2 \cdot 6H_2O$. Mo_3NiS_4/zeolites exhibited higher activity and selectivity than AHM + Ni/zeolites regardless of the zeolite type. Cluster **2** as a precursor is more suitable for preparing zeolite-supported Ni–Mo bimetallic catalysts than the combined use of AHM and $Ni(NO_3)_2 \cdot 6H_2O$. It is noteworthy that the selectivity for dihydrobenzothiophene was relatively high for the AHM + Ni/zeolite catalyst while on the cluster-derived catalysts the products that were simply hydrogenated without desulfurization were scarce. Table 7 indicates that Mo_3NiS_4/NaY and Mo_3NiS_4/KL showed similar activity; however, the latter showed much higher activity for the HDS of benzothiophene under high-concentration conditions (40).

The influence of the nickel addition method on the HDS reaction is shown in Table 8. Here the benzothiophene content in decane was increased 10 times to compare the activity of the nickel-promoted catalysts at relatively low conversions. The nickel-added catalyst Ni + Mo_3S_4/KL proved more active than Mo_3S_4/KL. Moreover, the selectivity for ethylbenzene remarkably increased at the expense of simply hydrogenated products; nickel added by ion exchange with Ni^{2+} acted as a good promoter for Mo_3S_4/KL. However, Mo_3NiS_4/KL exhibited much higher activity and selectivity for HDS than Ni + Mo_3S_4/KL although the electronic character of molybdenum and nickel in Mo_3NiS_4/KL and Ni + Mo_3S_4/KL was similar as revealed by XPS. The HDS activity and selectivity increased in the order: Mo_3S_4/KL < Ni + Mo_3S_4/KL < Mo_3NiS_4/KL; nickel addition was most effective when the nickel–molybdenum bimetallic sulfide cluster **2** was used. The retention of Ni–S–Mo linkage of the nickel–molybdenum cluster in Mo_3NiS_4/KL was revealed by EXAFS. Although the cubane-type structure of the nickel–molybdenum cluster would have changed by thermal treatment in He and the following HDS reaction, as described above, the initial uniformity of nickel and molybdenum with the Mo–S–Ni linkage could be kept and high dispersion of molybdenum species seems to result in producing HDS active sites very effectively. In contrast, Ni + Mo_3S_4/KL, in which no strong interaction of Ni and Mo was observed by EXAFS, led to less active catalyst upon pretreatment. The effectiveness of employing the Mo–Ni mixed cluster suggests that the cluster structure is reflected in the active species for HDS.

CONCLUSIONS

The molybdenum sulfide cluster and the nickel–molybdenum sulfide cluster have been successfully incorporated into zeolites with a 12-membered ring by aqueous ion exchange. The structure of the molybdenum cluster did not change during ion exchange. The complete cubane-type structure of the nickel–molybdenum cluster mostly remained after ion exchange but partly decomposed to Ni^{2+} and the molybdenum cluster by adventitious oxygen. All cluster-derived catalysts showed a higher conversion of benzothiophene than AHM-derived catalysts used after presulfiding. Mo_3S_4/KL and Mo_3S_4/NaMOR showed higher levels of activity for HDS of benzothiophene than other Mo_3S_4/zeolites. Regardless of the method of addition of nickel, the nickel-added catalysts were more active in the HDS reaction than the catalysts solely based on molybdenum; in particular, the selectivity for ethylbenzene remarkably increased at the expense of simply hydrogenated products. The catalysts prepared by ion-exchanging zeolites with nickel–molybdenum bimetallic sulfide cluster exhibited higher activity than the catalysts prepared by ion-exchanging Mo_3S_4-containing zeolite with nickel nitrate solution. This higher HDS activity could be due to the retention of Mo–S–Ni linkage originating from the Mo_3NiS_4 core.

ACKNOWLEDGMENT

We thank Professor K. Asakura, Faculty of Science, The University of Tokyo, for his support with the EXAFS analyses.

REFERENCES

1. Kabe, T., Ishihara, A., and Tajima, H., *Ind. Eng. Chem. Res.* **31**, 1577 (1992).
2. Ma, X., Sakanishi, K., and Mochida, I., *Ind. Eng. Chem. Res.* **33**, 218 (1994).
3. Prins, R., De Beer, V. H. J., and Somorajai, G. A., *Catal. Rev. Sci. Eng.* **31**, 1 (1989).
4. Startsev, A. N., *Catal. Rev. Sci. Eng.* **37**, 353 (1995).
5. Landau, M. V., Berger, D., and Herskowitz, M., *J. Catal.* **158**, 236 (1996).
6. Michaud, P., Lemberton, J. L., and Perot, J., *Appl. Catal. A* **169**, 343 (1998).
7. Leglise, J., Manoli, J. M., Potvin, C., Djega-Mariadassou, G., and Cornet, D., *J. Catal.* **152**, 275 (1995).
8. Cid, R., Llambias, F. J. G., Fierro, J. L. G., Lopez-Agudo, A., and Villasenor, J., *J. Catal.* **89**, 478 (1984).
9. Fierro, J. L. G., Conesa, J. C., and Lopez-Agudo, A., *J. Catal.* **108**, 334 (1987).
10. Okamoto, Y., Maezawa, A., Kane, H., and Imanaka, T., *J. Mol. Catal.* **52**, 337 (1989).
11. Abdo, S., and Howe, R. F., *J. Phys. Chem.* **87**, 1713 (1983).
12. Dai, P. E., and Lunsford, J. H., *J. Catal.* **64**, 173 (1980).
13. Johns, J. R., and Howe, R. F., *Zeolites* **5**, 251 (1985).
14. Huang, M., and Howe, R. F., *J. Catal.* **108**, 283 (1984).
15. Ward, M. B., Mizuno, K., and Lunsford, J. H., *J. Mol. Catal.* **27**, 1 (1984).
16. Cotton, F. A., Dori, Z., Llusar, R., and Schwotzer, W., *J. Am. Chem. Soc.* **107**, 6734 (1985).
17. Shibahara, T., Yamasaki, M., Sakane, G., Minami, K., Yabuki, T., and Ichimura, A., *Inorg. Chem.* **31**, 640 (1992).
18. Akashi, H., Shibahara, T., and Kuroya, H., *Polyhedron* **9**, 1671 (1990).
19. Taniguchi, M., Ishii, Y., Murata, T., Tatsumi, T., and Hidai, M., *J. Chem. Soc. Chem. Commun.*, 2533 (1995).
20. Kabe, T., Qian, W., and Ishihara, A., *J. Catal.* **149**, 171 (1994).
21. Shibahara, T., Akashi, H., and Kuroya, H., *J. Am. Chem. Soc.* **108**, 1342 (1986).
22. Dimmock, P. W., Lamprecht, G. J., and Sykes, A. G., *J. Chem. Soc. Dalton Trans.* 955 (1991).
23. Shibahara, T., Yamasaki, M., Akashi, H., and Katayama, T., *Inorg. Chem.* **30**, 2693 (1991).
24. Shibahara, T., Sakane, G., Naruse, Y., Taya, K., Akashi, H., Ichimura, A., and Adachi, H., *Bull. Chem. Soc. Jpn.* **68**, 2769 (1995).
25. Shibahara, T., Akashi, H., and Kuroya, H., *J. Am. Chem. Soc.* **110**, 3313 (1988).
26. Murata, T., Gao, H., Mizobe, Y., Nakano, F., Motomura, S., Tanase, T., Yano, S., and Hidai, M., *J. Am Chem. Soc.* **114**, 8287 (1992).
27. Murata, T., Mizobe, Y., Gao, H., Ishii, Y., Wakabayashi, T., Nakano, F., Tanase, T., Yano, S., Hidai, M., Echizen, I., Nanikawa, H., and Motomura, S., *J. Am. Chem. Soc.* **116**, 3389 (1994).
28. Wakabayashi, T., Ishii, Y., Murata., T., Mizobe, Y., and Hidai, M., *Tetrahedron Lett.* **36**, 5585 (1995).
29. Wakabayashi, T., Ishii, Y., Ishikawa, K., and Hidai, M., *Angew. Chem. Int. Ed. Engl.* **35**, 2123 (1996).
30. Louwers, S. P. A., and Prins, R., *J. Catal.* **133**, 94 (1992).
31. Delmon, B., *Ind. Eng. Chem.* **20**, 693 (1980).
32. Taniguchi, M., Ishii, Y., Murata, T., Hidai, M., and Tatsumi, T., *in* "Studies in Surface Science and Catalysis, Vol. 105, Progress in Zeolite and Microporous Materials" (H. Chon, S.-K. Ihm, and Y. S. Uh, Eds.), part B, p. 893. Elsevier, Amsterdam, 1997.
33. Jiang, M., and Tatsumi, T., *J. Phys. Chem. B* **102**, 10879 (1998).
34. Tatsumi, T., Taniguchi, M., Yasuda, S., Ishii, Y., Murata, T., and Hidai, M., *Appl. Catal.* **139**, L5 (1996).
35. Taniguchi, M., Yasuda, S., Ishii, Y., Murata, T., Hidai, M., and Tatsumi, T., "Proceedings, 11th International Congress on Catalysis, Baltimore, 1996" (J. W. Hightower, W. N. Delgass, E. Iglesia, and A. T. Bell, Eds.), Studies in Surface Science and Catalysis, Vol. 101, part A, p. 107. Elsevier, Amsterdam, 1996.
36. Taniguchi, M., Ishii, Y., Murata, T., Hidai, M., and Tatsumi, T., in preparation.
37. Meier, W. M., Olson, D. H., and Baerlocher, Ch., "Atlas of Zeolite Structure Types," 4th ed. Elsevier, New York, 1996.
38. Candia, R., Clausen, B. S., Bartholdy, J., Topsøe, N.-Y., Lengeler, B., and Topsøe, H., *in* "Proceedings, 8th International Congress on Catalysis, Berlin, 1984." p.II-375. Verlag Chemie, Weinheim, 1984.
39. Shido, T., and Prins, R., *J. Phys. Chem. B* **102**, 8426 (1998).
40. Tatsumi, T., Taniguchi, M., and Imamura, T., in preparation.